

which varies between 5 and 10% of the total beam current, whereas the enhanced MFC is relatively consistent and shows less than a 1.5% error in the measured beam current.

Even with the enhancements made to the MFC, the beam current is being underestimated by about 1% on average. This underestimation of the beam current is related to the width of the slits in the copper slit disk and the geometry of the beam trap, which still allows some backscattered electrons to escape from the cup. Reducing the slit widths of the copper slit disk and the diameter of the hole in the beam trap will further improve electron capture with the enhanced MFC if more precise beam current measurements are required from the MFC diagnostic.

The Effect of Slit Width on the Measured Power Density Distribution

The present version of the CT reconstruction algorithm assumes that the width of the slit is small compared to the diameter of the beam and can therefore be neglected. This assumption is reasonably valid for defocused beams where the ratio of slit width to beam diameter is small. However, for sharp-focused beams where the finite slit width represents a larger fraction of the beam's diameter, the diagnostic will overestimate the beam's diameter and thus underestimate the peak power density of the beam. The amount of error introduced by the finite width of the slit can be calculated for Gaussian distributed beams, which is useful for selecting the appropriate slit width for a given beam.

Since the amount of error in the measured power density distribution depends on both slit width and beam size, simulations were performed using sharp-focused beams to calculate the worst-case scenario (highest error introduced by a given slit) that we expect to measure with the CT diagnostic technique. Furthermore, since the beam size depends on accelerating voltage (Ref. 8) and electron optics, we measured the beam size for different accelerating voltages and on two different welding machines. These data are summarized in Table 2 for sharp-focused, 5-mA beams. Some of this data was previously obtained from Hamilton Standard EB welding machine No. 605 (Ref. 8), showing that the beam on this machine is full width at half maximum (FWHM) at 0.36 mm at 80 kV, and a smaller FWHM of 0.28 mm at 140 kV.

A similar comparison was made in the present investigation using Hamilton Standard welding machine No. 175. Figure 4 shows one result from this study,

Table 1 — Comparison of Measured Beam Current between Original MFC and Enhanced MFC for Different Beams

True Beam Current (mA)	Accelerating Voltage 1 60kV		Accelerating Voltage 2 140kV	
	Original MFC (mA)	Enhanced MFC (mA)	Original MFC (mA)	Enhanced MFC (mA)
5	4.77	4.98	4.75	4.90
10	9.34	9.91	9.35	10.0
15	14.1	14.8	14.1	14.8
19	17.8	18.7	16.4	18.8

EB Welding Machine HS No. 175.

Table 2 — Comparison of Measured Electron Beam Properties

Beam Property	EB Welding Machine No. 175		EB Welding Machine No. 605	
	60 kV	140 kV	80 kV	140 kV
Peak (kW/mm ²)	3.98	26.0	2.87	7.92
FWHM (mm)	0.26	0.15	0.36	0.28
l/e ² (mm)	0.42	0.26	0.61	0.45
(mm)	0.11	0.064	0.15	0.12

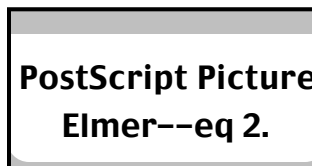
Note: Sharp-focused, 5-mA beams for two different welding machines and for different accelerating voltages.

comparing the tomographic reconstructions of the 60- and 140-kV beams. Here, the sharp-focused beams were measured to have a FWHM of 0.26 and 0.15 mm for the 60- and 140-kV voltages, respectively. For both welding machines, the beam became smaller as the voltage was increased, showing that higher voltage beams focus to smaller spot sizes than lower voltage beams for a given electron beam welding machine. In addition, the comparison between the two welding machines shows that HS welding machine No. 175 focuses to a smaller spot size than HS welding machine 605 at a given beam voltage.

The smallest measured beam size in this study was a 5-mA, 140-kV beam on HS No. 175, which had a CT-reconstructed FWHM of only 0.15 mm. This beam was chosen for the calculations that follow for estimating the maximum error introduced by the finite slit width into the CT reconstructions for these machines. In these calculations, the beam profile measured by the diagnostic is simulated by passing a Gaussian distributed beam over a slit of a given width. The error introduced by the finite width of the slit can then be calculated from the difference between the simulated beam profile and the true beam profile. This simulation assumes the electron beam has a circular Gaussian distribution that most closely represents the sharp-focused beam condition represented by the following equation (Ref. 9):

$$J(x, y) = \frac{I}{2\pi\sigma^2} \exp\left(-\frac{x^2}{2\sigma^2} - \frac{y^2}{2\sigma^2}\right) \tag{1}$$

where J(x,y) is the current density of the beam, σ is the standard deviation of the Gaussian distribution, I is the total beam current, and x and y are rectangular spatial coordinates. For a beam moving in the positive x-direction and perpendicular to the slit, the instantaneous current passing through the slit as a function of position, $I_S(x)$, can be calculated. This calculation is performed by integrating the current density distribution given by equation 1 along the y direction for a slit of width w as follows:



Equation 2 was integrated using Math-Cad (Ref. 12) for a series of simulated slit widths between 0.01 and 1 mm. This range of slit widths more than spans the range of slit widths used for electron beam tomography, which are typically on the order of 0.1 mm wide (Refs. 8, 9).

Figure 5A compares the results of three simulated beam profiles as the

using a ratio, R, of the slit width to the true FWHM of the beam. Here, the true FWHM of the beam is smaller than the beam profile measured using the MFC, which will be discussed in more detail later.

Simulations of beam profiles were made for a 0.15-mm FWHM beam using different slit widths up to the FWHM of the beam, i.e., for $0 < R < 1$. Figure 6 plots these results, showing a nonlinear increase in the error as R increases. The error in the measured FWHM of the beam can be quite large, exceeding 20% as the slit width approaches the FWHM of the beam, but drops off to values less than 5% for $R < 0.33$. These data were fit to a second order polynomial to determine a predictive relationship between R and the percentage error in the FWHM measurement, E_{FWHM} , as follows:

$$E_{FWHM}(\%) = 0.132 + 0.0061(R) + 25.2(R)^2 \quad (3)$$

where the variables $E_{FWHM}(\%)$ and R are defined as

$$E_{FWHM}(\%) = 100 * (\text{FWHM measured} - \text{FWHM true}) / \text{FWHM true} \quad (4)$$

$$R = (\text{slit width}) / (\text{FWHM true}) \quad (5)$$

Using these relationships, the percentage error introduced by tungsten slits of 0.1 and 0.2 mm were calculated for different beams. These slits represent the two different sizes used in the original tungsten slit disk design whereby 16 small slits (0.1 mm) and one large slit (0.2 mm) were used for beam orientation purposes. Four different beam sizes were investigated as well, representing two different accelerating voltages on HS Nos. 175 and 605 welding machines.

Table 3 summarizes the results of these calculations. In this table, the measured FWHM data are the FWHM values as experimentally determined from the CT reconstruction of the beam, while the true FWHM data are those required to produce the CT-reconstructed value for a given slit width.

The true FWHM value was back-calculated using an iterative procedure from the tomographically reconstructed (measured) FWHM of the beam, the slit width, and Equations 3-5. The error in the FWHM measurement represents the percentage that the CT reconstruction overestimates the true FWHM of the beam, as calculated from the difference between the true and measured FWHM values.

These results show the 0.1-mm-wide slit produces errors between 3.58 and 14.9%, while the double-wide slit pro-

Table 3 — Amount of Error in Measured FWHM Values of Sharp-Focused, 5-mA Beams as a Result of Different Slit Widths

EB Welding Machine	Voltage (kV)	Slit Width (mm)	Measured FWHM (mm)	True FWHM (mm)	R	Error (E_{FWHM}) (%)
No. 605	140	0.1	0.280	0.270	0.370	3.58
No. 175	60	0.1	0.260	0.250	0.400	4.12
No. 175	140	0.1	0.150	0.131	0.763	14.9
No. 605	140	0.2	0.280	0.237	0.843	18.0
No. 175	60	0.2	0.260	0.212	0.943	22.5
No. 175	140	0.2	0.150	0.074	2.70	102

Note: Results are from two different welding machine, and for different accelerating voltages.

duces significantly higher errors, between 18.0 and 102% in the FWHM of these different beams. It is clear the amount of error introduced into the FWHM measurement by the 0.2-mm-wide slit is excessive for small-diameter beams. Furthermore, the fact that not all the slits in the tungsten slit disk are the same size makes it difficult to properly compensate for the effect of slit width on the CT-reconstructed beam. Because of this potential error, we investigated a new method for orienting the beam using 17 small, uniform slit widths that would allow the amount of error in the CT reconstruction to be more accurately predicted.

Determining Beam Orientation Using Equal Width Slits

The original 17 slit tungsten disk design is illustrated in Fig. 7A. In this design, the slits are equally spaced at 21.18 deg, giving an equivalent spacing of 10.59 deg per beam profile in the reconstructed beam (Ref. 8). The beam orientation is determined using one wide slit (0.2 mm) (Ref. 8), which can produce a large error in the beam profile as discussed above.

The new tungsten slit design is illustrated in Fig. 7B. In this design, all of the slits are machined with the same width (0.1 mm) to reduce the amount of error introduced into the CT reconstruction, and the beam orientation is determined with one wide-spaced set of slits.

The spacing of the wide slit was chosen to be as small as possible to keep the overall spacing of the remaining slits as

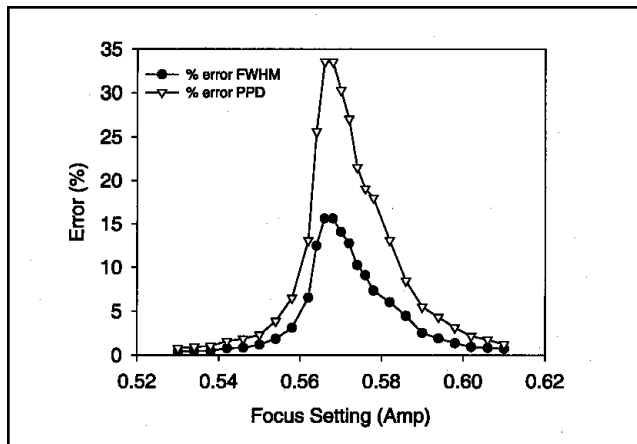


Fig. 9 — Percentage error in the FWHM and peak power density measurements caused by the 0.1-mm-wide slit as a function of focus setting for the 140-kV, 5-mA beam on HS welding machine No. 175.

regular as possible. Here, we chose 24 deg for the wide-spaced slit, which produced enough of a temporal gap in the acquired data waveform for the sharp-focused and defocused beams investigated in this study to be characterized.

The remainder of the slits were equally spaced at 21 deg. This nonregular slit spacing required only minor changes to be made to the CT algorithm for reconstructing the beam. Since this disk also contained 17 slits, the CT reconstruction was performed with the same average angular resolution as that of the original slit disk design.

Using the new tungsten slit disk design, a 140-kV, 5-mA beam was investigated through a range of focus settings of ± 0.040 A. This beam was shown to have a measured FWHM of 0.148 mm at sharp focus, which corresponds to a corrected true FWHM value of 0.128 mm. Waveform analysis of raw data was performed in preparation of tomographic reconstruction and showed the wide angle was able to be distinguished in the 17-slit waveform for both sharp-focused and defocused beams (± 0.040 A). Thus the

